PHYSICS OF FLUIDS VOLUME 14, NUMBER 9 SEPTEMBER 2002

Statistics of two-particle dispersion in two-dimensional turbulence

G. Boffetta
Dipartimento di Fisica Generale and INFM, Università di Torino via Pietro Giuria 1, 10125 Torino, Italy

I. M. Sokolov
Theoretische Polymerphysik, Universität Freiburg, Hermann-Herder Straße 3, D-79104 Freiburg i.Br., Germany and Institut für Physik Humboldt-Universität zu Berlin, Invalidenstraße 110, D-10115 Berlin, Germany

(Received 7 November 2000; accepted 12 June 2002; published 5 August 2002)

We investigate Lagrangian relative dispersion in direct numerical simulation of two-dimensional inverse cascade turbulence. The analysis is performed by using both standard fixed time statistics and an exit time approach. The latter allows a more precise determination of the Richardson constant which is found to be $g \simeq 4$ with a possible weak finite-size dependence. Our results show only small deviations with respect to the original Richardson's description in terms of diffusion equation. These deviations are associated with the long-range correlated nature of the particles' relative motion. The correlation, or persistence, parameter is measured by means of a Lagrangian "turning point" statistics. © *2002 American Institute of Physics.* [DOI: 10.1063/1.1498121]

I. INTRODUCTION

Understanding the statistics of particle pairs dispersion in turbulent velocity fields is of great interest for both theoretical and practical implications. At variance with single particle dispersion which depends mainly on the large scale, energy containing eddies, pair dispersion is driven (at least at intermediate times) by velocity fluctuations at scales comparable with the pair separation. Since these small scale fluctuations have universal characteristics, independent on the details of the large scale flow, relative dispersion in fully developed turbulence is expected to show universal behavior.[1,2] From an applicative point of view, a deep comprehension of relative dispersion mechanisms is of fundamental importance for a correct modelization of small scale diffusion and mixing properties.

Since the pioneering work by Richardson,[3] many efforts have been done to confirm experimentally or numerically his description.[2,4–10] Nevertheless, the main obstacle to a deep investigation of relative dispersion in turbulence remains the lack of sufficient statistics due to technical difficulties in laboratory experiments and to the moderate inertial range reached in direct numerical simulations.

In this paper we present a detailed investigation of the statistics of relative dispersion from extensive direct numerical simulations of particle pairs in two-dimensional Navier–Stokes turbulence. We will see that the main ingredient of the original Richardson description, i.e., Richardson diffusion equation, is sufficient for a rough description of relative dispersion in this flow. Nevertheless, our simulations show that, at least at finite Reynolds numbers, two-particle statistics is rather sensible to finite size effects. This demands for a different analysis based on doubling time statistics which has been recently introduced for the analysis of Lagrangian dispersion.[11] Comparison of numerical results with ones based on the Richardson's equation shows that the last delivers a qualitatively good description of the doubling-time-distributions. The quantitative deviations found are attributed to the fact that the dispersion process is not purely diffusive and is influenced by ballistic (persistent) motion.

The article is organized as follows: In Sec. II we discuss the Richardson's approach to the two-particle dispersion, in Sec. III the fixed-scale properties of dispersion process (such as doubling-time statistics) are considered. The numerical approach and the results of simulations are discussed in Sec. IV. Section V is devoted to conclusions. The mathematical details of calculations of doubling-time statistics for the Richardson's case are given in Appendices A and B.

II. STATISTICS OF RELATIVE DISPERSION

Relative dispersion in turbulence is often phenomenologically described in terms of a diffusion equation for the probability density function of pair separation $p(\mathbf{r},t)$

$$\frac{\partial p(\mathbf{r},t)}{\partial t} = \frac{\partial}{\partial r_i}\left(K_{i,j}(\mathbf{r},t)\, \frac{\partial p(\mathbf{r},t)}{\partial r_j}\right), \tag{1}$$

with a space and time dependent diffusion coefficient $K_{i,j}(\mathbf{r},t)^2$. The original Richardson proposal, obtained from experimental data in the atmosphere, corresponds to $K(r,t) = K(r) = k_0 \varepsilon^{1/3} r^{4/3}$, where ε has the dimension of energy dissipation (see below) and k_0 is a dimensionless constant. In the d-dimensional isotropic case, this diffusion equation takes the form

$$\frac{\partial p(\mathbf{r},t)}{\partial t} = \frac{1}{r^{d-1}}\, \frac{\partial}{\partial r}\, r^{d-1} K(r)\, \frac{\partial p(\mathbf{r},t)}{\partial r}. \tag{2}$$

Its solution leads to the well-known non-Gaussian distribution

$$p(\mathbf{r},t) = \frac{A}{(k_0 t)^3 \varepsilon} \exp\left(-\frac{9 r^{2/3}}{4 k_0 \varepsilon^{1/3} t}\right), \tag{3}$$

where A is a normalizing factor. The growth of pair separation is described in terms of a single exponent as

$$R^{2n}(t) \equiv \langle r^{2n}(t) \rangle = C_{2n} \varepsilon^n t^{3n}, \tag{4}$$

and the so-called Richardson constant is $g = C_2 = \frac{1280}{243} k_0^3$.

The Richardson's conjecture was formulated based on the scaling nature of the diffusion coefficient and in analogy with diffusion. No information about the nature of the pdf was available by that time. Any choice of the form $K(r,t) \simeq r^{4/3-\alpha} \langle r^2(t) \rangle^{\alpha/2}$ [i.e., $K(r,t) \simeq r^{4/3-\alpha} t^{3\alpha/2}$] would give the same scaling law $R^2 \propto t^3$ but with different pdf's (see Refs. 1, 2, 12–14).

The possibility to describe the dispersion process by means of a diffusion equation is based on essentially two important physical assumptions which can be verified *a posteriori*. The first one is that the dispersion process is self-similar in time, which is a reasonable assumption in the case of nonintermittent velocity field;[9] the second one is that the velocity field is short correlated in time.[15] Indeed, in the limit of velocity field δ-correlated in time the diffusion equation (1) becomes exact.[16,17] As we proceed to show, the Richardson's conjecture (2), which is exact under small values of the persistence parameter of the flow,[15,18] still delivers a qualitatively good approximation for realistic two-dimensional (2D) turbulent flows, whose persistence parameter of the order of 1.

Richardson scaling in turbulence is a consequence of Kolmogorov scaling for the velocity differences.[2] Under Kolmogorov scaling, the mean-square relative velocity and the correlation time in the inertial range are given by

$$\langle \delta v(r)^2 \rangle \simeq v_0^2 \left(\frac{r}{r_0} \right)^{2/3} \simeq \varepsilon^{2/3} r^{2/3} \tag{5}$$

and

$$\tau(r) \simeq \tau_0 \left(\frac{r}{r_0} \right)^{2/3} \simeq \varepsilon^{-1/3} r^{2/3}, \tag{6}$$

where r_0, τ_0, and v_0 are some (large scale) characteristic length, time, and velocity scale and $\varepsilon \simeq v_0^2/\tau_0$ is the energy flux in the inertial range. The value of the dimensionless combination $Ps = v_0 \tau_0 / r_0$ remains, however, unspecified by scaling considerations. It is referred to as a persistence parameter of the flow and plays a central role in describing single particle diffusion and pair separation.[15,18] The persistence parameter Ps introduced here is related to a Kubo number of Ref. 19. Note however, that in our case this parameter is scale-independent within the inertial range.

The persistence parameter gives the ratio of the velocity correlation time to the Lagrangian characteristic time. In order to see how Ps influences Lagrangian dispersion, let us consider the following simple model, which has been used as a basis for building a stochastic model of turbulent dispersion.[15] We take that the magnitude of the separation velocity (i.e., the projection of the velocity difference on the line connecting the particles) is a function of r only so that $\delta v(r) = v_0 (r/r_0)^{1/3}$. The temporal changes of the flow can be accounted for by letting the particle change its velocity direction from time to time, while keeping the velocity's magnitude constant. Let us consider the probability that the relative velocity of particle separation changes its direction during time interval dt (i.e., the probability that the trajectory of the relative motion has a turning point at the current particles' positions). Note that the corresponding probability density has a dimension of inverse time, and may depend on r. According to the scaling assumption the only corresponding form can be $dp \simeq dt/\tau(r)$. The growth of the magnitude of the interparticle separation $\mathbf{r}(t)$ in dt is $dr \simeq \delta v(r) dt$, thus the probability to change the direction of velocity within dr is, using (5) and (6)

$$dp = p(r) dr = \frac{dr}{\partial v(r) \tau(r)} = \frac{r_0}{v_0 \tau_0} \frac{dr}{r} = \frac{1}{Ps} \frac{dr}{r}. \tag{7}$$

The distribution of the position of turning points in the separation follows from (7).[18] The conditional probability density to find a next turning point at r_2 provided a previous one was at $r_1 < r_2$ is given by

$$\Psi(r_2 | r_1) = \frac{1}{Ps r_1} \left(\frac{r_2}{r_1} \right)^{-1/Ps - 1}. \tag{8}$$

Note that the dependence of $\Psi(r_2|r_1)$ only on the relative positions of the turning points, i.e., on r_2/r_1, is a clear consequence of scale invariance.

The tail of $\Psi(r_2|r_1)$ decides about the existence of the second moment of this distribution, i.e., on the fact whether the corresponding motion is short- or long-range correlated in space. Depending on the persistence parameter Ps, the dispersion can be either diffusive ($Ps \ll 1$) or ballistic ($Ps \gg 1$) in nature. In what follows (8) will be used as a definition of Ps. Note that the power-law tail of the distributions make the problem extremely sensitive to the finite-size effects, especially for large Ps, when the weights of ballistic events (Lévy-walks[20]) is considerable.

We note that the value of Ps is not a free parameter, but is fixed for a given physical situation. The scaling nature of turbulence supposes that this parameters is a constant, depending only on general properties of the flow, e.g., on its 2D or 3D nature (in this last case also the overall geometry of the flow can be of importance). On the other hand, since the nature of dispersion process depends crucially on the value of Ps, the only way for getting quantitative information about the dispersion is through direct numerical simulations or laboratory experiments. The strong finite-size effects in relative dispersion statistics call for the introduction of quantities which are less sensitive to finite resolution.

III. EXIT TIME STATISTICS

In general, statistical properties of fully developed turbulence can be observed only in high-Reynolds number flows in which the inertial range, where the scaling laws hold, is sufficiently wide. The needs for large Reynolds numbers is particularly severe in the case of Richardson dispersion, as a consequence of the long tails in the distribution (3). Moreover, the observation of time scaling laws as (4) requires sufficiently long times in order to forget the initial separation.[2]

For these reasons, the observation of Richardson scaling [i.e., (3) or (4)] is very difficult in direct numerical simulations where the Reynolds number is limited by the resolution. The same kind of limitations arise in laboratory experiments, as a consequence of the necessity to follow the Lagrangian trajectories which limits again the Reynolds number.[7,8]

To partially overcome these difficulties, an alternative approach based on *exit time* statistics has been recently proposed.[9,11] Given a set of thresholds $R_n = \rho^n R(0)$ within the inertial range, one computes the ''doubling time'' $T_\rho(R_n)$ defined as the time it takes for the particle pair separation to grow from threshold R_n to the next one R_{n+1}. Averages are then performed over many dispersion experiments, i.e., particle pairs, to get the mean doubling time $\langle T_\rho(R)\rangle$. The outstanding advantage of this kind of averaging at fixed scale separation, as opposite to a fixed time, is that it removes crossover effects since all sampled particle pairs belong to the same scales.

The problem of doubling time statistics is a first-passage problem for the corresponding transport process. For the Richardson case, in 2D it is given by the solution of the Richardson's diffusion equation, Eqs. (2), with initial condition $p(\mathbf{r},0) = \delta(r - R/\rho)/2\pi$ and absorbing boundary at $r = R$ [so that $p(R,t) = 0$]. The pdf of doubling time can be obtained as the time derivative of the probability that the particle is still within the threshold

$$p_D(t) = -\frac{d}{dt}\int_{|\mathbf{r}|<R} p(\mathbf{r},t)\,d\mathbf{r}. \tag{9}$$

Using (2) one obtains

$$p_D(t) = -2\pi\varepsilon^{1/3}k_0R^{7/3}\left.\frac{\partial p(\mathbf{r},t)}{\partial r}\right|_{r=R}. \tag{10}$$

The solution using the eigenfunction decomposition is given in Appendix A and shows that the long-time asymptotic of $p_D(t)$ is exponential

$$p_D(t) \simeq \exp(-\kappa k_0 \varepsilon^{1/3} R^{-2/3} t), \tag{11}$$

where $\kappa \approx 2.93$ is a number factor. This exponential nature of the tail of $p_D(t)$-distribution will be confirmed by direct simulations in Sec. IV.

Note that the combination $\varepsilon^{-1/3}R^{2/3}$ has a dimension of time and is proportional to the average doubling time $\langle T_\rho(R)\rangle$. This time can be obtained by a simple argument reported in Appendix B. In the two-dimensional case one obtains

$$\langle T_\rho(R)\rangle = \frac{3}{4}\,\frac{\rho^{2/3}-1}{\varepsilon^{1/3}\rho^{2/3}}\,\frac{R^{2/3}}{k_0}. \tag{12}$$

Prediction (12) contains the parameter k_0 which, as shown in Sec. II, is dependent on the Richardson constant g. As a consequence, the computation of average doubling time can be used for an alternative (and more robust, as we will see) estimation of g. It is convenient to rewrite the doubling time pdf (11) in terms of the average doubling time $\langle T_\rho(R)\rangle$. Making use of (12) one obtains in 2D the asymptotic expression

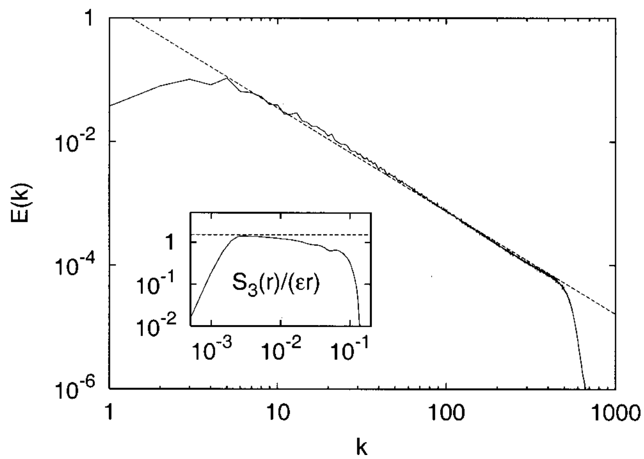

FIG. 1. Energy spectrum $E(k)$ of the inverse cascade simulations at resolution $N = 2048$ with random forcing around scale $l_f \simeq 0.0074$. The dashed line is the Kolmogorov spectrum $E(k) = C\varepsilon^{2/3}k^{-5/3}$ with $C = 6.0$. In the inset it is shown the compensated third-order longitudinal structure function $S_3(r)/(\varepsilon r)$ with the prediction 3/2 (dashed line).

$$p_D(t) \simeq \exp(-0.252t/\langle T_\rho(R)\rangle), \tag{13}$$

which is a parameterless, universal function.

IV. DIRECT NUMERICAL SIMULATIONS

Pair dispersion statistics has been investigated by extensive direct numerical simulations of the inverse energy cascade in two-dimensional turbulence.[21] There are several reasons for considering 2D turbulence. First of all, the dimensionality of the problem makes feasible direct-numerical simulations at high Reynolds numbers. Moreover, the observed absence of intermittency[22] makes the 2D inverse energy cascade an ideal framework for the study of Richardson scaling in Kolmogorov turbulence.

The 2D Navier–Stokes equation for the vorticity $\omega = \nabla \times \mathbf{v} = -\Delta\psi$ is

$$\partial_t\omega + J(\omega,\psi) = \nu\Delta\omega - \alpha\omega + \phi, \tag{14}$$

where ψ is the stream function and J denotes the Jacobian. The friction linear term $-\alpha\omega$ extracts energy from the system to avoid Bose–Einstein condensation at the gravest modes.[23] The forcing ϕ is active only on a typical small scale l_f and is δ-correlated in time to ensure the control of the energy injection rate. The viscous term has the role of removing enstrophy at scales smaller than l_f and, as customary, it is numerically more convenient to substitute it by a hyperviscous term (of order eight in our simulations). Numerical integration of (14) is performed by a standard pseudospectral method on a doubly periodic square domain of size $L = 2\pi$ at resolutions ranging from $N = 128$ up to $N = 2048$. All the results presented are obtained in conditions of stationary turbulence.

In Fig. 1 we plot the typical energy spectrum, which displays Kolmogorov scaling $E(k) = C\epsilon^{2/3}k^{-5/3}$ over about two decades with Kolmogorov constant $C \simeq 6.0$. In the inset we plot the third-order longitudinal structure function $S_3(r) = \langle \delta v(r)^3\rangle$ compensated with the theoretical prediction $S_3(r) = 3/2\varepsilon r$. The observation of the plateau confirms the

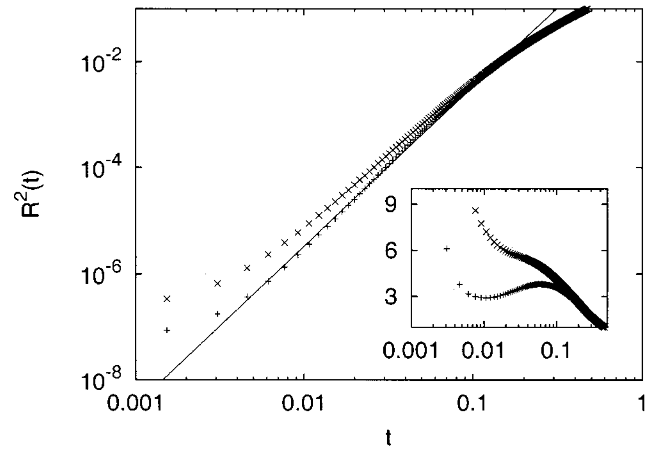

FIG. 2. Relative dispersion $R^2(t)$ with $R(0)=\delta x/2$ (+) and $R(0)=\delta x$ (×) and the Richardson law $R^2(t)=g\varepsilon t^3$ with $g=3.8$. In the inset the compensated plot $R^2(t)/(\varepsilon t^3)$ is displayed.

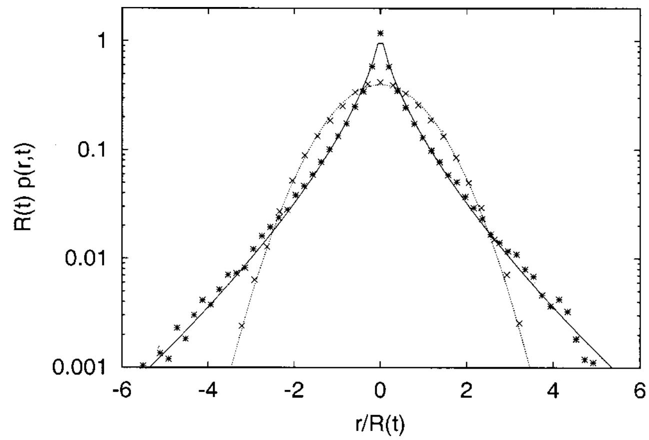

FIG. 3. Probability distribution function of relative separations at time $t=0.031$ (*) and $t=0.77$ (×) rescaled with $R(t)=\langle r^2(t)\rangle^{1/2}$. The continuous line is the Richardson prediction (3), the dashed line is the Gaussian distribution.

existence of an inverse energy cascade and indicates the extension of the inertial range. Previous numerical investigation has shown that velocity differences statistics in the inverse cascade is not affected by intermittency corrections.[22] In this case we may expect the Lagrangian statistics to be self-similar with Richardson scaling.[9]

Lagrangian statistics is obtained by integrating the trajectories of many (up to 64 000) particle pairs in the turbulent velocity field, initially uniformly distributed with constant separation $R(0)$.

The Lagrangian data reported below are in dimensionless units in which separations are rescaled with the box size L and time with the large scale time $T_0=(L^2/\varepsilon)^{1/3}$.

A. Relative dispersion analysis

In Fig. 2 we plot the relative dispersion $R^2(t)$ in the highest resolution simulations for two different initial separation, $R(0)=\delta x/2$ and $R(0)=\delta x$ (where $\delta x=2\pi/N$ is the grid mesh and $N=2048$). The Richardson t^3 law (4) is observed in a limited time interval, especially for the larger $R(0)$ run. Aymptotically, $R^2(t)$ is independent on the initial separation but it is remarkable that the relative separation law displays such a strong dependence on the initial conditions even in our high resolution runs.

This dependence makes the determination of the Richardson constant particularly difficult. In the inset of Fig. 2 we show the compensated plot $R^2(t)/t^3$ which, in the dimensionless units, should directly give the constant g. It is clear that a precise determination of g is impossible; even the Richardson scaling (4), when looked in a compensated plot, is rather poor. Figure 2 suggests that starting with an intermediate initial separation would give a wider scaling range. Of course, one would like to avoid this "fine tuning," which is probably impossible to implement in the case of experimental data. These effects are even more dramatic in the case of low resolution simulations (see Appendix C). In the following Section we will introduce a technique which avoids this problems.

The probability distribution function of pair separations is plotted in Fig. 3 for the $R(0)=\delta x/2$ run. At short time $t=0.015$, in the beginning of the t^3 range in Fig. 2, we found that the Richardson pdf (3) fits pretty well our data, although some deviations can be detected. Of course, at time comparable with the integral time $t=0.77$, particle separations are of the order of the integral scale and we observe Gaussian distribution. The crossover between these two regimes is extremely broad: Deviations from Richardson pdf are clearly seen already for the times well within the Richardson's t^3 range. To observe better this transition, in Fig. 4 we plot, in log–log plot, the right tail of $-\ln(p(r,t)/p(0,t))$. The far tails of $p(r,t)$ represent pairs at large separation which are first affected by finite-size effects. As a consequence, the slope of the tail can be fitted with an exponent α which change continuously in time, from 2/3 to the Gaussian value 2 (see the inset of Fig. 4). Thus self similarity, if it exists, is reduced to the very short time at the beginning of dispersion. Moreover, the scaling region is strongly affected by the choice of initial separation, as shown in Fig. 2.

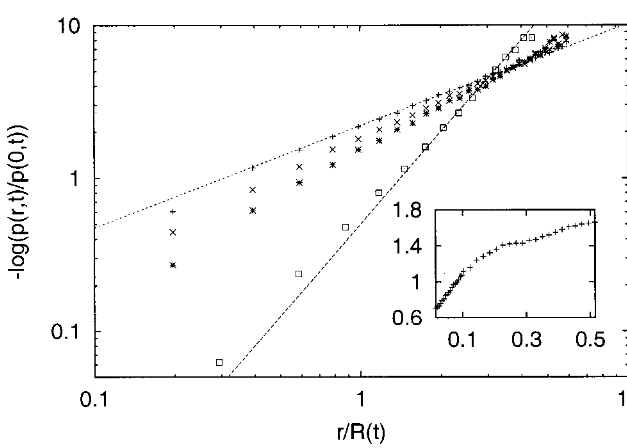

FIG. 4. Right tail of $-\log(p(r,t)/p(0,t))$ at times $t=0.015$ (+), $t=0.041$ (×), $t=0.067$ (*), and $t=0.77$ (□) in log–log plot. The two lines represent the Richardson slope 2/3 and the Gaussian slope 2. The inset shows the exponent of the right tail of the pdf as a function of time.

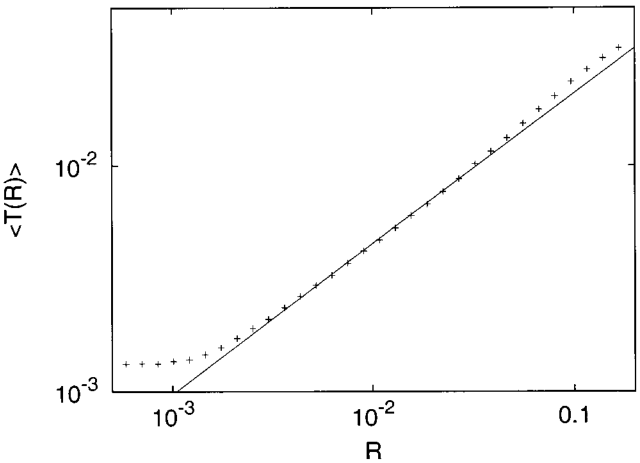

FIG. 5. Mean doubling time $\langle T(R)\rangle$ as function of the separation R. The ratio is $\rho=1.2$ and the average is obtained over about 5×10^5 events. The line represent the dimensional scaling $R^{2/3}$.

B. Doubling time data

The same Lagrangian trajectories discussed in the previous section have been used for computing exit time statistics. In Fig. 5 we plot the average doubling time for the $N=2048$ simulation together with the dimensional prediction $\langle T(R)\rangle \simeq R^{2/3}$. The improvement in the scaling of Fig. 5 with respect to Fig. 2 is evident thus allowing for a more precise determination of the constant. Let us also observe that, by definition, exit time statistics is independent on the initial separation $R(0)$ (as far as is it sufficiently small) thus the two realizations of Lagrangian trajectories shown in Fig. 2 give the same result.

In Fig. 6 we plot the quantity $\frac{20}{9}[(\rho^{2/3}-1)^3/\rho^2](R^2/\varepsilon\langle T\rangle^3)$ which from (4) and (12) gives the value of the Richardson constant, for different resolutions. As expected, the extension of the scaling region (i.e., the plateau in Fig. 6) increases with the resolution. In the inset we plot the so obtained value of g as a function of the forcing scale $k_f=2\pi/l_f$ (i.e., the extension of the inertial range). It is interesting to observe that the estimated value of g is significantly smaller at low resolution simulation. In the limit of high resolution the Richardson constant approaches the value $g \simeq 3.8$, although a residual weak dependence on resolution cannot be excluded.

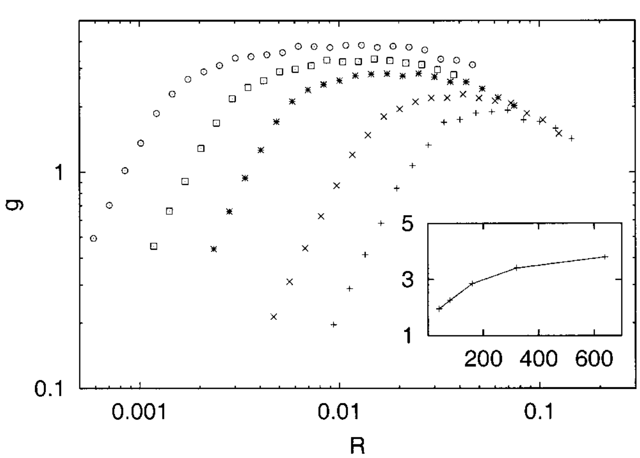

FIG. 6. Mean doubling time compensated as $(20/9)[(\rho^{2/3}-1)^3/\rho^2](R^2/\varepsilon\langle T\rangle^3)$ in order to give the Richardson constant g for different resolutions: $N=128$, $l_f=L/40$ (+), $N=256$, $l_f=L/80$ (×), $N=512$, $l_f=L/160$ (*), $N=1024$, $l_f=L/320$ (□) and $N=2048$, $l_f=L/640$ (○). In the inset the value of g as a function of l_f is plotted.

It is interesting to compare our result with previous estimations of g. The only experimental estimation of g for 2D inverse cascade[7] gives a value about seven times smaller, but the Reynolds number in the experiment is even smaller than in present simulations and thus finite size can have even more dramatic effects (see Appendix C). Other estimations of g are based on kinematic simulations with synthetic flows. In all these cases[5,6,24] the reported values are even smaller. In the case of kinematic simulations one has obviously $\varepsilon=0$ and g is defined by means of the Kolmogorov constant C. From this point of view, it is interesting to compare the 2D and 3D cases. Kolmogorov scaling requires $g\propto C^{3/2}$ and using the ratio $C_{2D}/C_{3D}\simeq 4.0^2$, one has that $g_{2D}/g_{3D}\simeq 8.0$. Thus, from this very crude argument (which, for example, do not take into account the role of the dimensionality), our finding $g_{2D}\simeq 3.8$ predicts $g_{3D}\simeq 0.48$ which is indeed very close to recent experimental[8] and numerical[25] results. It is also interesting to observe that our numerical finding is not far from the prediction of turbulence closure theory.[13,26]

From Fig. 5 we observe that at very small separations $R\simeq 10^{-3}$, the doubling time has a tendency to a constant value $\langle T(R)\rangle \simeq 0.0016$. On these scales we are below the forcing scale (see Fig. 1), and the velocity field can be assumed smooth. As a consequence of Lagrangian chaos we expect on these scales an exponential amplification of separations[27] at a rate given by the Lagrangian Lyapunov exponent λ. The latter can be obtained as $\lambda=\lim_{R\to 0}\ln\rho/\langle T(R)\rangle$[11] and gives $\lambda\simeq 110$ (in dimensionless units). The Lagrangian Lyapunov exponent λ is a small scale quantity (i.e. depends on the Reynolds number of the simulation), and thus has to be compared with a small scale characteristic time. One can estimate the smallest characteristic time $\tau_{\min}$ by the minimum value of $(k^3E(k))^{-1}$. We obtain $\lambda\simeq 0.23\tau_{\min}^{-1}$.

In Fig. 7 we plot the doubling time pdf $p_D(T)$ compensated with the mean value $\langle T(R)\rangle$ at different scales in the inertial range $0.003\leqslant R\leqslant 0.046$. First, we obtain a very nice collapse of the different curves, indicating that relative dispersion in two-dimensional turbulence, when looked in the correct way, is a self similar process. Second, we observe the exponential tail predicted in Sec. III with a fitted coefficient 0.3 which is indeed not far from the theoretical prediction (13) based on the Richardson's picture. The difference between the predicted and measured values of the prefactors is not large, but perceptible: It shows that the Richardson's equation gives a correct qualitative description of the dispersion process, but is not exact. The reasons for deviations from the diffusive picture proposed by Richardson are the long-range correlations in the particles' motion, as seen from the analysis of the turning points of their relative trajectories.

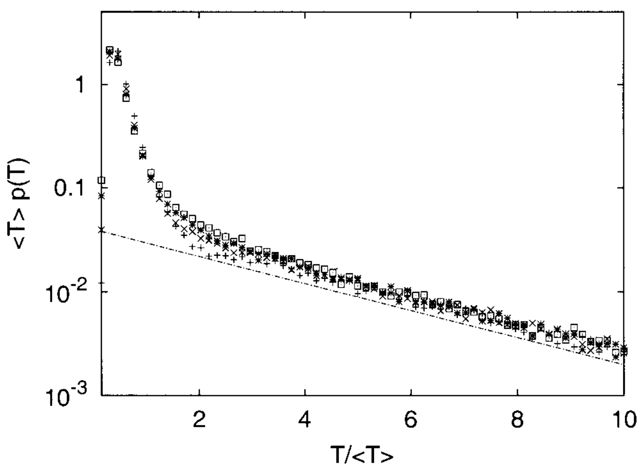

FIG. 7. Pdf of doubling times at resolution $N=2048$ for distances $R=0.003$ (+), $R=0.075$ (×), $R=0.02$ (*) and $R=0.046$ (□). The dashed line is the exponential $\exp(-0.3T/\langle T\rangle)$.

C. Turning points statistics and the persistence parameter

A possible explanation for the deviations of our high-resolution numerical data from the Richardson's picture is the not very small value of the persistence parameter. As discussed in Sec. II, at large values of Ps the contribution of ballistic events may lead to non-Richardson distributions and moreover makes the dispersion strongly sensible to finite-size effects, cutting the longer trajectories.

We have computed the persistence parameter making use of (8). We have recorded, for each pair, the set of turning points r_i at which the pair's relative velocity changes sign. From the set of r_i we have then computed the pdf of the ratio r_{i+1}/r_i, accumulating for all the i and all the pairs. The result, plotted in Fig. 8, gives $Ps\simeq 0.87$. The requirement that both r_1 and r_2 are in the inertial range, strongly limits the statistics on turning points and the numerical result is affected by rather large uncertainty. Nevertheless, it is remarkable that the power law tail in the conditional probability density $\Psi(r_2|r_1)$ is well observed in our numerical simulations. This justifies, a posteriori, the use of models based on $\Psi(r_2|r_1)$ for describing relative dispersion.[15] The numerical value of the effective persistence parameter $Ps\simeq 0.87$ is not so small, and can explain the observed deviations from Richardson pdf (which are, however, less pronounced in a 2D flow than in a theoretical one-dimensional model[18]): The transport in a 2D turbulent flow is neither purely diffusive nor ballistic.[28]

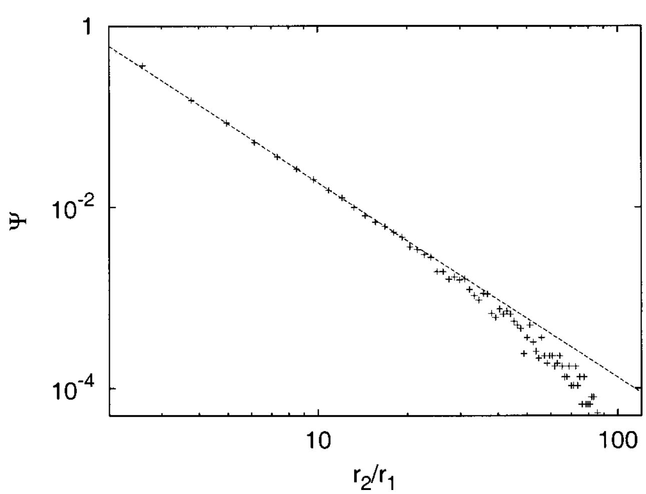

FIG. 8. Probability density function of turning point ratio $\Psi(r_2/r_1)$. The exponent of the power law (dashed line) gives the value $P_s\simeq 0.87$.

In order to be more confident on the numerical value of Ps obtained through the turning-points statistics, let us show that it agrees with a simple estimates based on the values of the Kolmogorov's and the Richardson's constants. According to the Kolmogorov's scaling, the mean squared relative velocity of the pair is given by

$$\langle \delta v^2(r)\rangle = C_2 \varepsilon^{2/3} r^{2/3}, \tag{15}$$

with $C_2\simeq 13$.[22] If the particles separate ballistically with the rms velocity

$$\delta v(r) = C_2^{1/2} \varepsilon^{1/3} r^{1/3}, \tag{16}$$

the distance between them should grow as

$$R_{\max}^2 = \left(\frac{2}{3}\right)^3 C_2^{3/2} \varepsilon t^3. \tag{17}$$

On the other hand, due to the unsteadiness of the separation velocity, the distance between the particles grows slower, namely as $R^2 = g\varepsilon t^3$, so that the factor

$$\xi^2 = R^2/R_{\max}^2 = \left(\frac{3}{2}\right)^3 \frac{g}{C_2^{3/2}}, \tag{18}$$

serves as a measure of this unsteadiness and ξ^2 is connected with the value of the persistence parameter. In our case, $\xi^2 \approx 0.28$. Within the stochastic model of Ref. 18 this corresponds to a value of Ps between 1.1 and 1.2, in reasonable agreement with the direct measurement from the turning-point statistics, and again corroborates the stochastic approach.

We also note a possibility to "tune" the Ps value by performing simulations in which the Lagrangian trajectories are integrated according to $\dot{\mathbf{x}} = \lambda \mathbf{v}(\mathbf{x},t)$. By changing the value of parameter λ one effectively changes v_0 and thus Ps. In the extreme case $\lambda\to 0$ the trajectories resemble those in a time δ-correlated velocity field. In the opposite limit, $\lambda \gg 1$ we have dispersion in a quenched field. Of course, it is only for the standard value $\lambda=1$ that Lagrangian trajectories move consistently with velocity field (i.e., for $\nu=\alpha=\phi=0$ (14) conserves vorticity along the Lagrangian trajectories). For other values of λ such simulations suffer the typical problem of advection in synthetic field (i.e., wrong reproduction of the sweeping effect, see Ref. 9 for a discussion). Simulations for several values of λ show that existence of the power-law tails of $\Psi(r_2|r_1)$ is a robust effect, as supposed by the model of Refs. 15 and 18, and that Ps grows with λ. As an example, in Fig. 9 we plot the probability density $\Psi(r_2|r_1)$ obtained from a simulation with $\lambda=0.5$. All the Eulerian parameters are the same of Fig. 8. We again observe a clear power law tail but now with $Ps\simeq 0.58$.

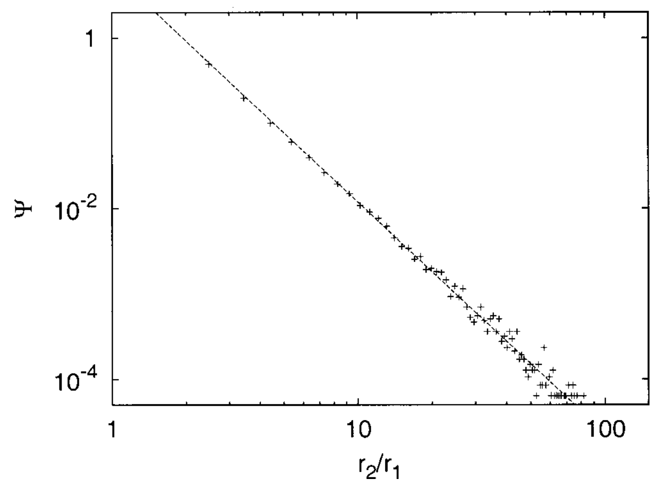

FIG. 9. The same of Fig. 8 but for $\lambda=0.5$. The persistence parameter is now $P_s \simeq 0.58$.

V. CONCLUSIONS

We have investigated the Lagrangian relative dispersion in direct numerical simulation of two-dimensional turbulence. The inverse energy cascade of two-dimensional turbulence displays Kolmogorov scaling without intermittency and it is thus the natural framework for investigating possible deviations from the classical Richardson picture.

The analysis of the numerical data was performed by using both standard statistics at fixed time and exit time statistics at fixed scale. The latter is shown to be more robust in finite Reynolds situations. An application of exit time statistics is developed for measuring the Richardson constant with good accuracy. The numerical result obtained $g \simeq 3.8$ is possibly still affected by weak finite-size effects, at is it shown by comparison with simulations at different resolutions.

We have studied the distribution of particle pair separations in the spirit of Richardson's diffusion equation. The rather large deviations (with respect to Richardson theory) observed in the tails of the pdf at fixed times are mostly related to crossover effects due to finite Reynolds numbers and disappear when looking at exit time statistics. Thus, the Richardson's equation gives a good basis for qualitative description of the dispersion in turbulent flows.

Paying attention to the turning points of the relative trajectories allows for estimating the effective persistence parameter of the motion which is found to be of the order of unity. Thus, the motion shows a relevant ballistic component and is not purely diffusive. Nevertheless, the correlations are not too strong to fully destroy the Richardson's picture. This observation can be a starting point for further theoretical considerations.

We note that the methodology of analysis proposed here based on the fixed-scale statistics and on the analysis of the relative trajectories can be also applied to the analysis of laboratory experiments. It would be extremely interesting to see whether in this way one can reduce the disagreement with the simulations and obtains a consistent picture of relative dispersion in two-dimensional turbulence.

ACKNOWLEDGMENTS

We gratefully acknowledge the support of the DFG through SFB428, of the Fonds der Chemischen Industrie and of MURST (Contract No. 2001023848).

We thank M. Cencini, J. Klafter, and S. Musacchio for useful discussions. We acknowledge the allocation of computer resources from INFM Progetto Calcolo Parallelo.

APPENDIX A: THE PDF OF DOUBLING TIMES

Let us discuss the probability density $p_D(t)$ of the time when the a pair of particles initially at distance R/ρ separates up to the distance R, and obtain its asymptotic decay of this probability for t large.

Changing to a variable $\xi=(k_0\varepsilon^{1/3})^{-1/2}r^{1/3}$ reduces (2) to a radial part of a spherically symmetric diffusion equation with constant diffusion coefficient. In $2d$ one has

$$\frac{\partial p}{\partial t}=\frac{1}{9\xi^5}\frac{\partial}{\partial \xi}\xi^5\frac{\partial}{\partial \xi}p, \tag{A1}$$

with the initial condition $p(\xi,0)=\delta(\xi_{\min}-\xi)$ with $\xi_{\min}=(k_0\varepsilon^{1/3})^{-1/2}(R/\rho)^{1/3}$ and with the boundary condition $p(\xi_{\max},t)=0$, with $\xi_{\max}=(k_0\varepsilon^{1/3})^{-1/2}R^{1/3}$.

The solution of a boundary-value problem for (A1) can be obtained by means of eigenfunction decomposition. Assuming the variable separation we get the solution in the form $p(\xi,t)=\Sigma_i e^{-\lambda_i^2 t}\psi_i(\xi)$, where $\psi_i(\xi)$ is an eigenfunction of the equation

$$\frac{1}{9\xi^5}\frac{\partial}{\partial \xi}\xi^5\frac{\partial}{\partial \xi}\psi_i=-\lambda_i^2\psi_i, \tag{A2}$$

satisfying the boundary condition $\psi(\xi_{\max})=0$. The corresponding solution which is nonsingular in zero is $\psi_i=\xi^{-2}J_2(3\lambda_i\xi)$ (J_2 is the Bessel function[29]). The fact that ψ vanishes at $\xi_{\max}$ gives $3\lambda_i\xi_{\max}=j_{2,i}$, where $j_{2,i}$ is the i-the real zero of $J_2(x)$. For example, the smallest eigenvalue is $\lambda_1^2=j_{2,1}^2/9\xi_{\max}^2\approx 2.93k_0\varepsilon^{1/3}R^{-2/3}$. Since the projection of the initial condition onto the eigenfunction corresponding to this eigenvalue does not vanish, the long-time asymptotic of the doubling-time distribution is $\exp(-2.93k_0\varepsilon^{1/3}R^{-2/3}t)$.

APPENDIX B: AVERAGE DOUBLING TIME

The mean doubling time can be obtained from a stationary solution of the Richardson diffusion equation. Imagine that one particle per unit time is introduced at $r=R/\rho$ and there are, respectively, a reflecting and absorbing boundaries at $r=0$ and $r=R$. The stationary solution of (2) in 2D with the appropriate boundary conditions and continuity are R/ρ is

$$p(r)=\begin{cases} C[\rho^{4/3}-1] & \text{for } 0<r<R/\rho \\ C\left[\left(\frac{r}{R}\right)^{-4/3}-1\right] & \text{for } R/\rho<r<R \end{cases}. \tag{B1}$$

The number of particle in $r<R$ is

$$N=\int_{|\mathbf{r}|<R}p(r)d\mathbf{r}=2\pi\int_0^R rp(r)dr \tag{B2}$$

By using (B1) one obtains

$$N=2\pi C(1-\rho^{-2/3})R^2. \quad (B3)$$

The current at $r=R$, i.e., the number of particle exiting from the boundary R per unit time, is given, as in (10), as

$$J=-2\pi\varepsilon^{1/3}k_0R^{7/3}\left.\frac{\partial p(r)}{\partial r}\right|_{r=R}=\frac{8\pi}{3}C\varepsilon^{1/3}k_0R^{4/3}. \quad (B4)$$

The mean doubling time is the average time spent by a particle at $r<R$. It is given by the ratio N/J and thus

$$\langle T_\rho(R)\rangle=\frac{3}{4}\,\frac{\rho^{2/3}-1}{\varepsilon^{1/3}k_0\rho^{2/3}}R^{2/3}, \quad (B5)$$

which is Eq. (12).

APPENDIX C: FINITE-SIZE EFFECTS

In this appendix we briefly discuss the effect of finite resolution on the evaluation of relative dispersion. Let us consider an incompressible turbulent flow with inertial range defined on scales $l_f<r<L$. In the case of 2D turbulence l_f represents the forcing scale and L the integral scale, while in the 3D case they are the dissipative and the forcing scales, respectively. The velocity field is thus assumed smooth [i.e., $\langle \delta v(r)^2\rangle\sim r^2$] for $r<l_f$, Kolmogorov-type [i.e., $\langle \delta v(r)^2\rangle \sim r^{2/3}$] in the inertial range and saturates [$\langle \delta v(r)^2\rangle =2\langle v^2\rangle$] at the integral scale. The separation between two particles placed at initial distance $R(0)<l_f$ grows exponentially as long as it remains below the inertial range. In the inertial range the Richardson scaling $R^2(t)\sim t^3$ is expected. For $R(t)>L$ the behavior depends on the boundary conditions: In the present case of numerical simulations with periodic boundary conditions standard diffusive behavior $R^2(t)=2Dt$ is expected.

It is evident that a clear t^3 law can be observed only if $L\gg l_f$, i.e., in the case of high-Reynolds number flows. Otherwise, detailed numerical simulations performed with synthetic velocity field[9,11] have shown that the broad crossover from the exponential regime and to the diffusive regime can completely hide the intermediate inertial range regime.

An example of this effect is given in Fig. 10 which shows the behavior of $R^2(t)$ for low resolution simulation with $l_f=L/10\simeq 0.63$ for two different initial separations $R(0)$. The apparent t^3 regime is spurious, in the sense that it is not related to Kolmogorov velocity scaling but it is simply an artifact induced by the crossover from the exponential to the diffusive regime. As a consequence, the value of the Richardson constant computed from the compensated plot strongly depends on the initial separation [from $g\simeq 0.3$ to $g\simeq 0.5$ for $R(0)=0.005L$ to $R(0)=0.01L$].

In Fig. 11 the result of the computation of mean doubling time is presented. The two lines represent the exponential and diffusive regimes and no Richardson $R^{2/3}$ regime is observed (compare with Fig. 5). Thus, also in this case of extremely low resolution, the advantage of doubling time statistics for the interpretation of Lagrangian data is evident.

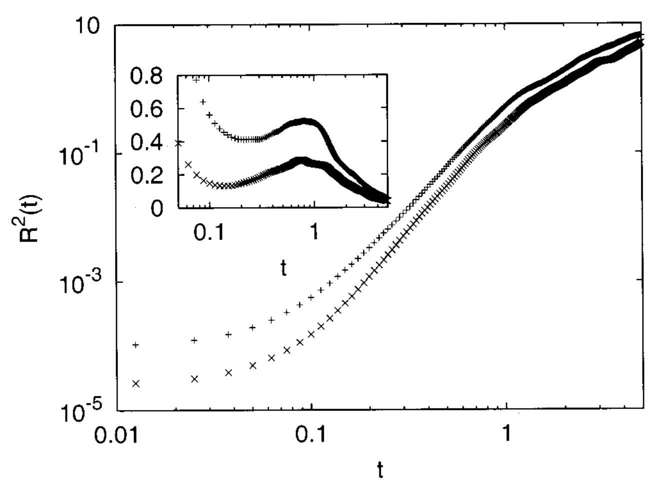

FIG. 10. Relative dispersion $R^2(t)$ for the low resolution simulation with $l_f=L/10$ at initial separations $R(0)=l_f/10$ and $R(0)=l_f/20$. In the inset the compensated plot $R^2(t)/(\varepsilon t^3)$ is shown.

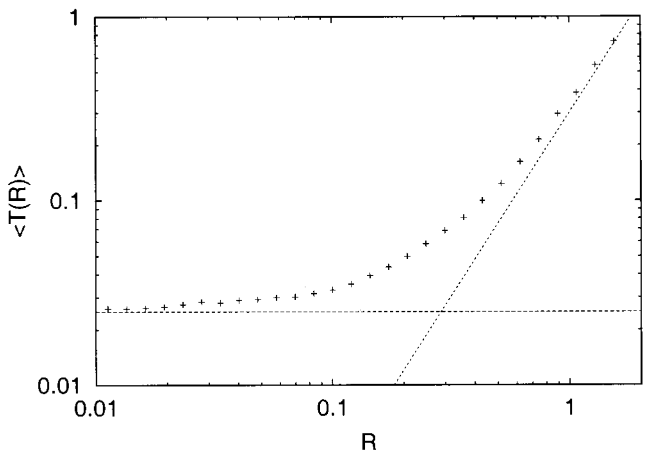

FIG. 11. Mean doubling time $\langle T(R)\rangle$ as function of the separation R for the same simulation of Fig. 10. The dashed line represent the exponential regime, the dotted line the diffusive regime $\langle T(R)\rangle\simeq R^2$.

[1] G. K. Batchelor, "Diffusion in a field of homogeneous turbulence II: The relative motion of particles," Proc. Cambridge Philos. Soc. **48**, 345 (1952).
[2] A. Monin and A. Yaglom, *Statistical Fluid Mechanics* (MIT Press, Cambridge, MA, 1975), Vol. 2.
[3] L. F. Richardson, "Atmospheric diffusion shown on a distance-neighbour graph," Proc. R. Soc. London, Ser. A **110**, 709 (1926).
[4] N. Zovari and A. Babiano, "Derivation of the relative dispersion law in the inverse energy cascade of two-dimensional turbulence," Physica D **76**, 318 (1994).
[5] F. W. Elliott, Jr. and A. J. Majda, "Pair dispersion over an inertial range spanning many decades," Phys. Fluids **8**, 1052 (1996).
[6] J. C. H. Fung and J. C. Vassilicos, "Two-particle dispersion in turbulent-like flows," Phys. Rev. E **57**, 1677 (1998).
[7] M. C. Jullien, J. Paret, and P. Tabeling, "Richardson pair dispersion in two-dimensional turbulence," Phys. Rev. Lett. **82**, 2872 (1999).
[8] S. Ott and J. Mann, "An experimental investigation of the relative diffusion of particle pairs in three-dimensional turbulent flow," J. Fluid Mech. **422**, 207 (2000).
[9] G. Boffetta, A. Celani, A. Crisanti, and A. Vulpiani, "Pair dispersion in synthetic fully developed turbulence," Phys. Rev. E **60**, 6734 (1999).
[10] G. Boffetta and A. Celani, "Pair dispersion in turbulence," Physica A **280**, 1 (2000).
[11] V. Artale, G. Boffetta, A. Celani, M. Cencini, and A. Vulpiani, "Dispersion

of passive tracers in closed basins: Beyond the diffusion coefficient,'' Phys. Fluids **9**, 3162 (1997).

[12] A. Okubo, ''A review of theoretical models for turbulent diffusion in the sea,'' J. Oceanogr. Soc. Jpn., **20**, 286 (1962).

[13] R. Kraichnan, ''Dispersion of particle pairs in homogeneous turbulence,'' Phys. Fluids **9**, 1728 (1966).

[14] H. G. E. Hentschel and I. Procaccia, ''Relative diffusion in turbulent media: The fractal dimension of clouds,'' Phys. Rev. A **29**, 1461 (1984).

[15] I. M. Sokolov, ''Two-particle dispersion by correlated random velocity fields,'' Phys. Rev. E **60**, 5528 (1999).

[16] R. Kraichnan, ''Small-scale structure of a scalar field convected by turbulence,'' Phys. Fluids **11**, 945 (1968).

[17] G. Falkovich, K. Gawedzki, and M. Vergassola, ''Particle and fields in fluid turbulence,'' Rev. Mod. Phys. **73**, 913 (2001).

[18] I. M. Sokolov, J. Klafter, and A. Blumen, ''Ballistic versus diffusive pair dispersion in the Richardson regime,'' Phys. Rev. E **61**, 2717 (2000).

[19] M. Vlad, F. Spineanu, J. H. Misguich, and R. Balescu, ''Collisional effects on diffusion scaling laws in electrostatic turbulence,'' Phys. Rev. E **61**, 3023 (2000).

[20] M. F. Shlesinger, B. West, and J. Klafter, ''Lévy dynamics of enhanced diffusion: Application to turbulence,'' Phys. Rev. Lett. **58**, 1100 (1987).

[21] R. H. Kraichnan and D. Montgomery, ''Two-dimensional turbulence,'' Rep. Prog. Phys. **43**, 547 (1980).

[22] G. Boffetta, A. Celani, and M. Vergassola, ''Inverse energy cascade in two-dimensional turbulence: Deviations from Gaussian behavior,'' Phys. Rev. E **61**, R29 (2000).

[23] L. M. Smith and V. Yakhot, ''Bose condensation and small-scale structure generation in a random force driven 2D turbulence,'' Phys. Rev. Lett. **71**, 352 (1993).

[24] J. Fung, J. Hunt, N. Malik, and R. Perkins, ''Kinematic simulation of homogeneous turbulence by unsteady random Fourier modes,'' J. Fluid Mech. **236**, 281 (1992).

[25] G. Boffetta and I. Sokolov, ''Relative dispersion in fully developed turbulence: The Richardson's law and intermittency corrections,'' Phys. Rev. Lett. **88**, 094501 (2002).

[26] M. Larcheveque and M. Lesieur, ''The application of eddy-dumped Markovian closures to the problem of dispersion of particle pairs,'' J. Mec. **20**, 113 (1981).

[27] A. Crisanti, M. Falcioni, G. Paladin, and A. Vulpiani, ''Lagrangian chaos: Transport, mixing and diffusion in fluids,'' Riv. Nuovo Cimento **14**, 1 (1991).

[28] N. A. Malik and J. C. Vassilicos, ''A Lagrangian model for turbulent dispersion with turbulent-like flow structure: Comparison with direct numerical simulation for two-particle statistics,'' Phys. Fluids **11**, 1572 (1999).

[29] *Handbook of Mathematical Functions*, edited by M. Abramovitz and I. A. Stegun (Dover, New York, 1972).